Physics-Based RTD Current-Voltage Equation

J. N. Schulman, H. J. De Los Santos, *Senior Member, IEEE,* and D. H. Chow

***Abstract*—An analytic expression for the current-voltage characteristics of resonant tunneling diodes is derived from basic principles. The form is ideal for insertion into circuit simulation models. It is demonstrated for a conventional InGaAs/AlAs RTD and for an InAs/AlSb/GaSb RIT diode. The expression is based on the quantum tunneling formalism and contains parameters that originate from physical quantities, but which can also be treated as empirical. Empirical fitting is straightforward and results in an excellent match to the data. Additional levels of physical realism can be incorporated in a natural way.**

I. Introduction

PROOF-OF-CONCEPT demonstrations of the application of resonant tunneling diodes (RTD's) to analog and digital circuits have been extensively documented in recent years [1]–[6]. This activity reflects the level of maturity achieved by RTD fabrication technology. To predict and explain circuit behavior, as well as to aid in selecting from the wide variety of RTD device structures/materials possibilities available, attempts to incorporate the RTD negative resistance into circuit simulation models have begun, usually based on SPICE-type CAD tools. Examples and further references can be found in [7].

A number of empirical RTD models have been advanced but they are basically curve fitting procedures which are loosely [4] or not at all [8]–[10] based on the underlying device physics. Consequently, the fits achieved are either crude for the simpler models, or involve increasingly complex forms to achieve a better match with data. We have discovered that there is a natural expression derived directly from the quantum model which is simple and gives an excellent fit to the data. The expression contains physical quantities which can also be treated as empirical parameters for fitting purposes, as is done in this paper. This framework is flexible and allows the incorporation of increasing levels of physical realism. At this point the formalism is suitable for circuit design, but not device design. The eventual goal would be to provide a framework for device design by relating the parameters to device choices such as layer widths, doping profiles, and material composition.

II. Derivation

Coon and Liu [11] (see also [4]) devised a simple model for negative resistance in the zero temperature limit. Our approach extends this to include the essential features of nonzero temperature and Fermi–Dirac statistics. We start from the standard formula [12] for the current in the effective mass approximation:

$$J = \frac{em^*kT}{2\pi^2\hbar^3}\int_0^\infty dE T(E,V) \cdot \ln\left[\frac{1+e^{(E_F-E)/kT}}{1+e^{(E_r-E-eV)/kT}}\right]$$

$$T(E,V) = \frac{\left(\frac{\Gamma}{2}\right)^2}{\left[E-\left(E_r-\frac{eV}{2}\right)\right]^2+\left(\frac{\Gamma}{2}\right)^2}.$$

The transmission coefficient is approximated by a Lorentzian. E is the energy measured up from the emitter conduction band edge. E_r is the energy of the resonant level relative to the bottom of the well at its center. Γ is the resonance width. This formula assumes equal width barriers and that half the voltage drop falls from the emitter to the center of the well. This assumption is not always valid. For better generality $eV/2$ can be replaced here and in the following equations by eVn with n determined from analysis or fitting.

For small Γ, the transmission coefficient is negligible except when E is close to the resonance, i.e., $E \cong E_r - eV/2$. Calculations show that Γ is on the order of one meV or less for even quite thin barrier widths [13]. This is much less than kT at room temperature. Therefore the substitution $E = E_r - eV/2$ can reasonably be made in the log term and it can be taken outside the integral. The integral is simple and the result is:

$$J = \frac{em^*kT\Gamma}{4\pi^2\hbar^3}\ln\left[\frac{1+e^{(E_F-E_r+eV/2)/kT}}{1+e^{(E_F-E_r-eV/2)/kT}}\right] \cdot \left[\frac{\pi}{2}+\tan^{-1}\left(\frac{E_r-\frac{eV}{2}}{\frac{\Gamma}{2}}\right)\right].$$

This formula can be regarded as providing the correct *form* for the lineshape, but calculated in an oversimplified way. The physical quantities can be allowed to depart from their actual values so as to compensate for the approximations and omissions in the model. The following form is the result:

$$J_1(V) = A\ln\left[\frac{1+e^{(B-C+n_1V)e/kT}}{1+e^{(B-C-n_1V)e/kT}}\right] \cdot \left[\frac{\pi}{2}+\tan^{-1}\left(\frac{C-n_1V}{D}\right)\right].$$

So far this form produces a peak current and a negative resistance, but there is no increasing valley current, which is due to tunneling through other channels and inelastic

Manuscript received October 16, 1995; revised December 22, 1995.

J. N. Schulman and D. H. Chow are with Hughes Research Laboratories, Malibu, CA 90265 USA.

H. J. De Los Santos is with the Hughes Space and Communications Company, Los Angeles, CA 90009 USA.

Publisher Item Identifier S 0741-3106(96)03734-2.

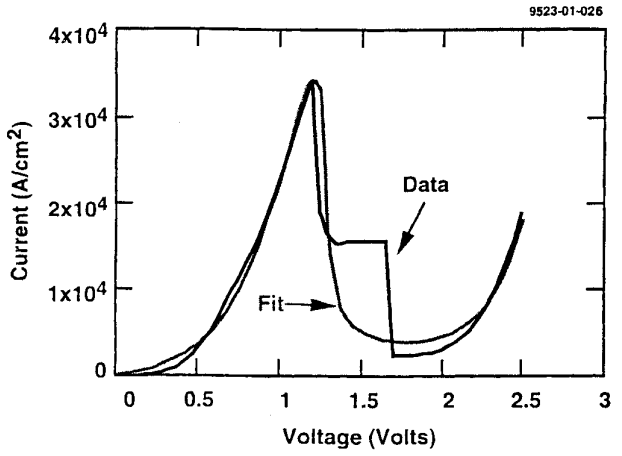

Fig. 1. Comparison of measured InGaAs/AlAs RTD I(V) and model fit.

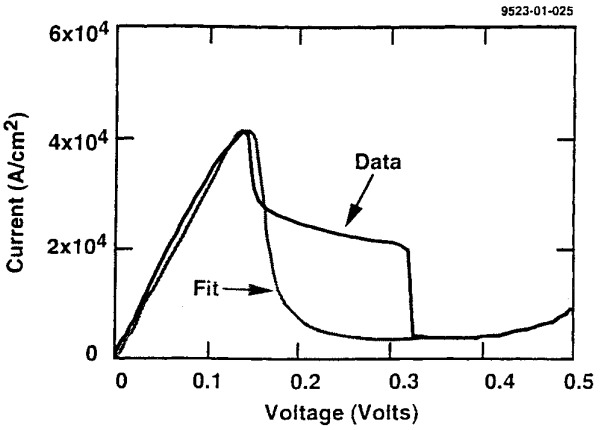

Fig. 2. Comparison of measured InAs/AlSb/GaSb RIT diode I(V) and model fit.

scattering. The simplest way to include a valley current contribution is to give it the form of tunneling through a higher resonance or thermal excitation over a barrier. For voltages below this higher energy channel, the additional current takes on the familiar diode form $J_2(V) = H(e^{n_2 eV/kT} - 1)$. Second or higher resonances can also be explicitly included if desired, using additional terms similar to J_1.

III. Results

Fig. 1 shows a comparison between measured data and a least squares fit using the sum $J(V) = J_1(V) + J_2(V)$. The RTD is made from $In_{0.53}Ga_{0.47}As$/AlAs with 26 Å barriers and a 48 Å well. 265 Å lightly doped spacer layers were sandwiched by highly doped contact layers. The fitting parameters used were $A = 10^4$, $B = 0.035$, $C = 0.1472$, $D = 0.0052$, $n_1 = 0.115$, $H = 1.411 \times 10^{-1}$, $n_2 = 0.1201$. The fit is excellent. In particular, the low voltage turn on, the peak width and shape, and the form of the valley current are all well reproduced. The plateau structure between the peak and the valley is known to be due to oscillations in the negative resistance region and not the true DC characteristic.

A second example, for an InAs/AlSb/GaSb resonant interband tunneling (RIT) diode, is shown in Fig. 2. It has 11 Å AlSb barriers and a 54 Å GaSb well. The sample had 420 Å spacer layers. RIT diodes differ in that the resonant state is light holelike, which has a negative effective mass. The above derivation assumes that the resonant state has a positive mass and thus is not directly applicable to this case. Despite this, Fig. 2 does indeed also demonstrate an excellent fit. It can be seen to be capable of producing the characteristic RIT attributes of low peak voltage, wide valley, and linear behavior at small voltage. The fitting parameters used were $A = 10^4$, $B = 0.0456$, $C = 0.0689$, $D = 0.0051$, $n_1 = 0.430$, $H = 1.43$, $n_2 = 0.4373$. The success of this fit for the RIT case is probably due to the delta-function-like nature of the Lorentzian which selects out only the electrons very close to the resonance regardless of whether it has positive or negative mass. However, further analysis is needed.

Here we demonstrate the application of the I–V formula by presenting results of a simple SPICE simulation for a third

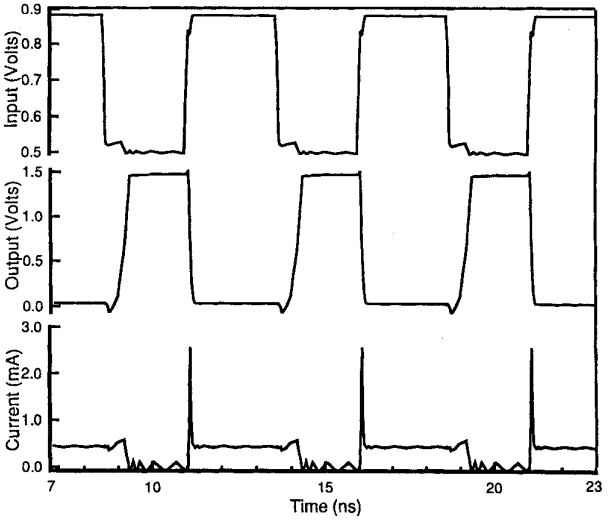

Fig. 3. InGaAs/InAlAs HBT-driver/RTD-load bipolar inverter transient analysis response.

RTD, made from InGaAs/InAlAs. This sample was chosen for its low series resistance and was not optimized for high speed performance. Fig. 3 shows the results for a HBT-driver/RTD-load bipolar inverter simulated using SPICE3f5 [7]. The RTD is modeled by a resistance in series with a parallel combination consisting of a nonlinear dependent current source and a nonlinear capacitor. For the RTD capacitance, the functional form $C_{jo}/(1 + |V|/V_{bi})^M$, with $C_{jo} = 0.03$ pF, $V_{bi} = 0.0368$ V, and $M = 0.19$ was used, where the parameters were obtained from a fit to capacitance calculations based on our self-consistent numerical two-band model [14]. Fig. 3 displays a plot of the inverter's transient response.

IV. Refinements

The values for the parameters $n_{1,2}$ above serve to stretch out the voltage scale. In actuality, there is a significant voltage drop over the collector spacer layer which causes most of the stretching [15]. This is not explicitly included in the above derivation, but is mimicked by the low values for $n_{1,2}$

used for the InGaAs/AlAs RTD. The band bending can be a large effect, especially if the spacer layer is wide and its doping small. The formula can be made more realistic by adding in an explicit simple form for the band bending in the total depletion approximation. Then, it can be included as a series voltage drop. The total depletion approximation gives $V_c = \varepsilon\varepsilon_0 F^2/2eN_d$ for the collector voltage drop. F is the electric field and is just V/d, where d is the thickness of the barriers and wells together. This result just has the form $V_c = \beta V^2$. The total voltage across the device is then $V_t = V + V_c$. The new parameter β can be used as a replacement for or in addition to n_1, which should return to a more physically realistic value. Note that the small voltage range of the RIT diode (Fig. 2) means that this refinement is not necessary, consistent with the fact that n_1 and n_2 are much closer to the ideal value of 0.5.

There are additional physical effects which the above formulas omit at present, but which can be incorporated with only minor modifications. For example, the dependence of the transmission peak on voltage has been ignored. The simple formula $T_{\max} = \sqrt{1-(eV/2E_r)^2}$ gives an excellent approximation for the decrease of the Lorentzian transmission peak to zero as the applied bias approaches the resonance condition and it can be incorporated in the above [16]. This is an illustration of how the physics based origin of this approach provides the flexibility to incorporate additional physical effects when desired. Although additional parameters are thereby introduced, paradoxically the effort to fit the data decreases and becomes *less* arbitrary, due to the increased physical realism.

V. Conclusion

We have developed a framework for bridging the gap between quantum mechanical models of resonant tunneling, circuit simulation models, and measured data. The formula we have derived involves variables which can be regarded as representing their true physical values, or these values can be considered to be starting points for an empirical fit. Additional physical effects can be added in as necessary in a realistic way [16].

References

[1] F. Capasso, S. Sen, A. Y. Cho, and D. Sivco, "Resonant tunneling devices with multiple negative differential resistance and demonstration of three-state memory cell for multiple-valued memory applications," *IEEE Electron Device Lett.*, vol. EDL-8, pp. 297–299, 1987.

[2] S. J. Wei, H. C. Lin, R. C. Potter, and D. Shupe, "A self-latching A/D converter using resonant tunneling diodes," *IEEE J. Solid-State Circuits,* vol. 28, no. 6, pp. 697–700, 1993.

[3] A. C. Seabaugh, A. H. Taddiken, E. A. Beam, III, J. N. Randall, Y.-C. Kao, and B. Newell, "Room-temperature resonant tunneling bipolar transistor XNOR and XOR integrated circuits," *Electronic Letts.,* vol. 29, no. 20, pp. 1802–1803, 1993.

[4] C. E. Chang, P. M. Asbeck, K. C. Wang, and E. R. Brown, "Analysis of heterojunction bipolar transistor/resonant tunneling diode logic for low-power and high-speed digital applications," *IEEE Trans. Electron Devices,* vol. 40, pp. 685–691, 1993.

[5] Z. X. Yan and M. J. Deen, "A new resonant-tunnel diode-based multivalued memory circuit using a MESFET depletion load," *IEEE J. Solid-State Circuits,* vol. 27, no. 8, pp. 1198–1202, 1992.

[6] J. Shen, G. Kramer, S. Tehrani, H. Goronkin, and R. Tsui, "Static random access memories based on resonant interband tunneling diodes in the InAs/GaSb/AlSb material system," *IEEE Electron Device Lett.,* vol. 16, no. 5, pp. 178–180, 1995.

[7] S. Mohan, J. P. Sun, P. Mazumder, and G. I. Haddad, "Device and circuit simulation of quantum electronic devices," *IEEE. Trans. Computer-Aided Design,* vol. 14, no. 6, pp. 653–662, 1995.

[8] T.-H. Kuo, H. C. Lin, U. Anandakrishnan, R. C. Potter, and D. Shupe, "Large-signal resonant tunneling diode model for SPICE3 simulation," *IEDM Tech. Dig.,* pp. 567–570, 1989.

[9] L. J. Michel and M. J. Paulus, "Differential multiple-valued logic using resonant tunneling diodes," in *Proc. 20th Int. Symp. Multiple-Valued Logic,* Charlotte, NC, May 1990, pp. 189–195.

[10] Z. Yan and M. J. Deen, "New RTD large-signal DC model suitable for PSPICE," *IEEE Trans. Computer-Aided Des. Integrated Circuits and Systems,* vol. 14, no. 2, pp. 167–172, Feb. 1995.

[11] D. D. Coon and H. C. Liu, "Frequency limit of double barrier resonant tunneling oscillators," *Appl. Phys. Lett.,* vol. 49, pp. 94–96, 1986.

[12] R. Tsu and L. Esaki, "Tunneling in a finite superlattice," *Appl. Phys. Lett.,* vol. 22, pp. 562–564, 1973.

[13] D. H. Chow, J. N. Schulman, E. Özbay, and D. M. Bloom, "1.7-ps, microwave integrated-circuit-compatible InAs/AlSb resonant tunneling diodes," *Appl. Phys. Lett.,* vol. 61, pp. 1685–1687, 1992 (see Table I).

[14] J. N. Schulman, "$Ga_{1-x}Al_xAs$-$Ga_{1-y}Al_yAs$-GaAs double-barrier structures," *J. of Appl. Phys.,* vol. 60, pp. 3954–3958, 1986; J. N. Schulman and M. Waldner, "Analysis of second level resonant tunneling diodes and transistors," *J. of Appl. Phys.,* vol. 63, pp. 2859–2861, 1988.

[15] M. Cahay, M. McLennan, S. Datta, and M. S. Lundstrom, "Importance of space-charge effects in resonant tunneling devices," *Appl. Phys. Lett.,* vol. 50, pp. 612–614, 1987.

[16] J. N. Schulman, in preparation.